

## Research Article

# Laccase Inhibition by Mercury: Kinetics, Inhibition Mechanism, and Preliminary Application in the Spectrophotometric Quantification of Mercury Ions

J. Juárez-Gómez,<sup>1</sup> E. S. Rosas-Tate,<sup>2</sup> G. Roa-Morales,<sup>2</sup> P. Balderas-Hernández,<sup>2</sup> M. Romero-Romo,<sup>3</sup> and M. T. Ramírez-Silva<sup>1</sup> 

<sup>1</sup>Departamento de Química, Universidad Autónoma Metropolitana Iztapalapa,

Área de Química Analítica, San Rafael Atlixco 186, Col. Vicentina, Iztapalapa, 09340 Ciudad de México, Mexico

<sup>2</sup>UAEMex, Centro Conjunto de Investigación en Química Sustentable CCIQS, UAEM-UNAM,

Universidad Autónoma del Estado de México, Carretera Toluca-Atzacmulco, km 14.5, 50200 Toluca, MEX, Mexico

<sup>3</sup>Departamento de Materiales, Universidad Autónoma Metropolitana-Azcapotzalco, Av. San Pablo 180, Col. Reynosa-Tamaulipas, Azcapotzalco, 02200 Ciudad de México, Mexico

Correspondence should be addressed to M. T. Ramírez-Silva; [mtrs218@xanum.uam.mx](mailto:mtrs218@xanum.uam.mx)

Received 13 March 2018; Accepted 8 May 2018; Published 4 June 2018

Academic Editor: Murat Senturk

Copyright © 2018 J. Juárez-Gómez et al. This is an open access article distributed under the Creative Commons Attribution License, which permits unrestricted use, distribution, and reproduction in any medium, provided the original work is properly cited.

The noncompetitive inhibition of laccase by mercury ions is reported, in particular focusing their effect over the enzyme catalytic activity. The enzymatic kinetics were obtained for different substrates (caffeic acid, gallic acid, and catechol), where caffeic acid displayed the greatest enzymatic activity. The laccase inhibition by mercury ions permitted to establish the inhibition effect through a mixed model (that actually displayed a behavior closer to that of the noncompetitive inhibitors) when evaluated by means of UV-Vis spectrophotometry, using caffeic acid as an electron donor. A mercury concentration of 2 mM led to 35% enzymatic inhibition after only a 2-minute incubation period. This method was used for quantification of mercury ions in aqueous solution, showing a detection limit of  $15 \pm 1$  ppm. Therefore, this work presented a novel perspective for the determination of the toxic Hg(II) ions that can be readily implemented into environmental remediation methods.

## 1. Introduction

Laccase is a multicopper enzyme commonly found in plants, fungi, and bacteria [1]; this enzyme is related to diverse functions, such as lignin synthesis and plant protection structures, sporulation, lignin degradation, and pathogenesis (fungi), of the mentioned organisms [2, 3]. The laccases have been studied for possible applications in the paper industry, due to their lignin degradation capacity [4], as well as in the treatment of wastewater contaminated by phenolic compounds [5]. This enzyme also has the capacity to oxidize polyphenols, diamines, and other types of compounds [6]. The transformation of the substrate is carried out by means of redox processes of the copper atoms distributed in three catalytic centers: type 1, strong absorption in the visible region  $\epsilon > 3,000 \text{ M}^{-1} \cdot \text{cm}^{-1}$  at 600 nm, spectrum of EPR with

$A_{\parallel} < 95 \times 10^{-4} \text{ cm}^{-1}$ ; type 2 or normal center, undetectable UV absorption, line of the EPR having a typical shape corresponding to low molecular weight Cu complexes; and type 3 or coupled binuclear center, strong absorption in the near UV with  $\lambda_{\text{max}} = 330 \text{ nm}$ , with no EPR signal, which occurs through coupling of the two antiferromagnetic copper ions [7, 8]. These catalytic centers have been characterized by means of electron paramagnetic resonance (EPR) [8, 9].

The measurement of the enzymatic activity and the inhibiting effects should lead to a betterment of the biologic catalyst knowledge and its possible applications in the near future. There are certain organic and inorganic compounds that inhibit the enzymatic activity, such as  $\text{Mn}^{2+}$ ,  $\text{Hg}^{2+}$ ,  $\text{Co}^{2+}$ , and  $\text{Cd}^{2+}$ , sulfates, nitrates and chlorides, fatty acids, sulfhydryl groups, quaternary ammonium detergents, and cysteine [10–12].

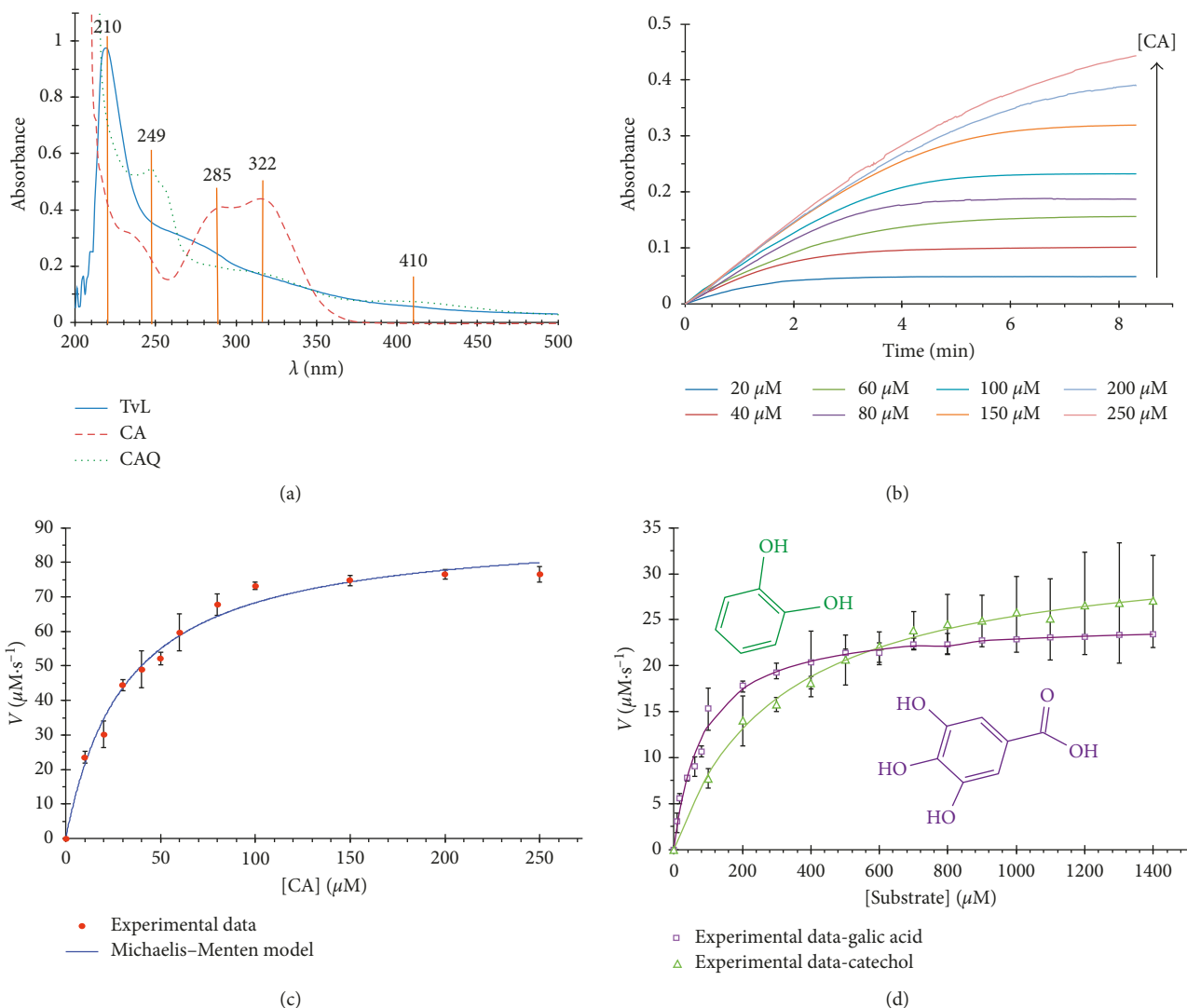


FIGURE 1: (a) Absorption spectra of the TvL, CA, and CAQ; (b) absorbance as a function of time for the oxidation reaction of different CA concentrations ( $\lambda = 410$  nm); (c) spectrophotometric determination of the Michaelis-Menten kinetics for CA oxidation by TvL; (d) spectrophotometric determination of the Michaelis-Menten kinetics for GA and CT oxidation by TvL. All tests were carried out at ambient temperature in acetate buffer (0.1 M, pH 4.5).

The presence of these metal ions in the environment has dangerously damaged it and given rise to various harmful effects to human health, all of them sharing a common anthropogenic origin, since they derive from mining and coal burning industrial activities [13]. Mercury exists in various forms: inorganic (ionic and metallic), to which humans are exposed to as an occupational hazard, and organic (ethylmercury, methylmercury, and phenylmercury, mainly). These forms differ in their degree of toxicity and the effects on the nervous, digestive, and immunologic systems, as well as on lungs, kidneys, skin, and eyes [14–16].

Several mercury(II) ion inhibition studies have been reported using various enzymes, such as laccase (*Daedalea quercina*, *Leptographium qinlingensis*), where mercury turned out to be the most potent inhibitor, attaining up to 98% inhibition at an ion concentration of 10 mM [10, 11]; cellulose (*Schizophyllum commune*), which exhibits high sensibility toward mercury and modifies the spectrophotometric

features of the enzyme [17]; invertase (yeast), which gives a larger inhibition respect to  $\text{Ag}^+$  ions and an inhibition from  $10^{-7}$  M [18];  $\alpha$ -amylase (*Paecilomyces variotii*), which displays a relative activity of 77% when adding a 10 mM  $\text{Hg}^{2+}$  concentration [19]; 5-aminolevulinic dehydratase acid (corn), where the mercury(II) ions modify the affinity toward the substrate and reaction rate, with the results based on the evaluation of  $K_m$  and  $V_{\max}$  [20]; and xylanase (*Trichoderma inhamatum*), which displays an enzymatic activity of 14.4% (2 mM) and 4.0% (10 mM) for xylanase type 1, as well as an activity of 15.6% (2 mM) and 5.9% (10 mM) mercury(II) [21].

This work presents the results concerning the spectrophotometric study of laccase from *Trametes versicolor* with three different substrates (caffeic acid, gallic acid, and catechol), evaluating their activity and inhibition degrees in the presence of mercury(II), and observing that millimolar mercury concentrations can reduce the laccase reaction extent. The assessment of the enzymatic activity and the

effects of the inhibitors will allow a better knowledge of the biologic catalyst and its possible future applications, like the indirect quantification of the inhibitor itself.

## 2. Materials and Methods

Laccase from *Trametes versicolor* (EC 1.10.3.2), with an activity of 13.6 U/mg, was obtained from Sigma; sodium acetate trihydrate was from JT Baker; acetic acid glacial was from Laboratorios Lutz, México, 60.05%; caffeic acid, gallic acid, and catechol were from Fluka; ethanol was from Sigma-Aldrich (HPLC degree);  $\text{Hg}(\text{NO}_3)_2$  was from Sigma-Aldrich; and deionized water was from a MilliQ Millipore equipment.

**2.1. Kinetic Analyses and Enzymatic Inhibition.** The kinetic UV-Vis tests were carried out in a Perkin Elmer Spectrometer Lambda 20. The absorbance of the caffeic acid oxidation was monitored at 410 nm using different substrate concentrations (10–250  $\mu\text{M}$ ); the catechol oxidation absorbance was monitored at 390 nm with different substrate concentrations (100–1400  $\mu\text{M}$ ); the gallic acid oxidation absorbance was monitored at 385 nm with different substrate concentrations (100–1400  $\mu\text{M}$ ). The  $\text{Hg}(\text{II})$  concentrations for laccase inhibition were 0.05, 0.1, 0.5, 1, 2, 3, and 4 mM. The incubation times for inhibition were 2, 5 and 10 contact minutes. The laccase concentration was 10  $\mu\text{g}\cdot\text{mL}^{-1}$  for all cases. All tests were carried out at ambient temperature in 1 cm optical path quartz cells in an acetate buffer (0.1 M pH 4.5). The experimental conditions were chosen based on studies reported by our working group [22, 23].

## 3. Results and Discussion

The laccase is considered a nonspecific enzyme, capable of oxidizing a wide variety of phenolic compounds, which is why this work used substrates like the caffeic acid, gallic acid, and catechol for the kinetic studies.

The system was characterized through UV-Vis spectroscopy from 800 to 200 nm; the results are shown in Figure 1(a): it can be observed that *Trametes versicolor* laccase (TvL) displayed two maximum absorption bands at 210 and 275 nm, whereas the caffeic acid (CA) shows three maximum absorption bands at 241, 285, and 322 nm. The (CA) oxidation product (caffeoquinone, labeled as CAQ) presents three absorption maxima at 250, 322, and 410 nm. The signal of the CAQ at 410 nm allows quantifying the enzymatic reaction product to enable the kinetic studies without interferences. The remaining substrates were also characterized as well as the oxidation products: the catechol (CT) exhibited two absorption bands with maxima at 227 and 270 nm, while the *o*-quinone (Q) presents a maximum absorption at 390 nm. The gallic acid (GA) showed only one maximum absorption band at 260 nm, and its oxidation product showed absorption maxima at 256 and 395 nm.

Figure 1(b) shows the absorbance at 410 nm as a function of time for different CA concentrations. It can be observed that, for each CA concentration, the absorbance increases linearly until attaining reaction equilibrium, where the absorbance remains constant; the time to reach equilibrium

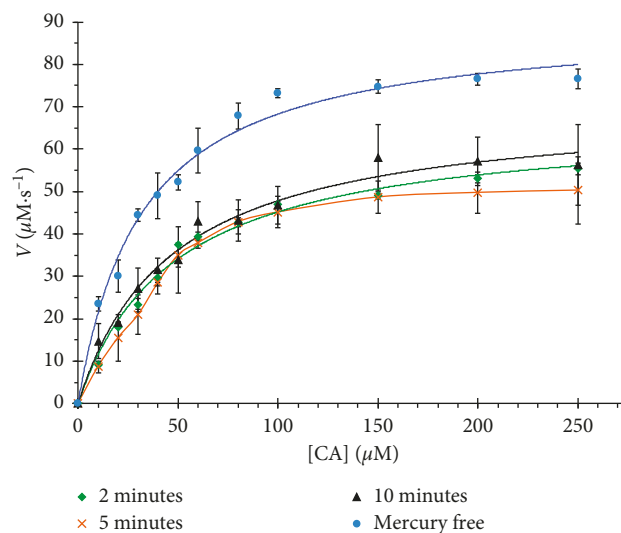


FIGURE 2: Spectrophotometric determination of the Michaelis–Menten kinetics for the CA oxidation by TvL in 1 mM mercury ion concentrations at different incubation times. The kinetics were determined in acetate buffer (0.1 M, pH 4.5), monitoring the CA enzymatic oxidation at 410 nm.

TABLE 1: Kinetic constants for different inhibition times of TvL by mercury(II), monitoring the CAQ absorbance at 410 nm in acetate buffer ( $n = 3$ ).

Inhibition time (minutes)	$K_m$ ( $\mu\text{M}$ )	$V_{\max}$ ( $\mu\text{M}\cdot\text{s}^{-1}$ )	$K_{\text{cat}}$ ( $\mu\text{MmL}\cdot\mu\text{g}^{-1}$ )	$k_{\text{cat}}/K_m$ ( $\text{mL}\cdot\mu\text{g}^{-1}$ )
0	$43 \pm 4$	$90 \pm 3$	$9.0 \pm 0.3$	$0.28 \pm 0.03$
2	$55 \pm 5$	$53 \pm 2$	$5.3 \pm 0.2$	$0.10 \pm 0.01$
5	$58 \pm 7$	$51 \pm 3$	$5.1 \pm 0.3$	$0.09 \pm 0.04$
10	$57 \pm 5$	$56 \pm 3$	$5.6 \pm 0.3$	$0.10 \pm 0.03$

increases with the substrate concentration, although it can be stated that at 8 minutes, all concentrations reached equilibrium. Furthermore, it is also observed that the slope of the linear segment increases with substrate concentration up to 100  $\mu\text{M}$ , where the said slope ceases to increase, indicating enzymatic saturation. The slope of the linear segments in these kinetic plots represents the absorbance change as a function of time; hence, in accordance with the Lambert–Beer law [24], the slope represents also a concentration change of the reaction product as a function of time, in other words, the enzymatic reaction rate.

Figure 1(c) shows the results of fitting the Michaelis–Menten kinetic model into the initial enzymatic reaction rate as a function of the CA concentration [25–29], giving a  $K_m = 43 \pm 4 \mu\text{M}$  and a  $V_{\max} = 90 \pm 3 \mu\text{M}\cdot\text{s}^{-1}$ . Figure 1(d) shows the initial enzymatic reaction rate as a function of the GA and CT concentration also with the Michaelis–Menten fitting; the kinetic constants obtained for these substrates were  $85 \pm 1 \mu\text{M}$  and  $307 \pm 18 \mu\text{M}$ , respectively, whereas the maximal rates were  $24 \pm 7$  and  $33 \pm 6 \mu\text{M}\cdot\text{s}^{-1}$ . These results indicate that the TvL exhibits a greater affinity toward CA since the  $K_m$  for this substrate is the smallest. Notwithstanding the saturation for the GA and CT happened at higher substrate concentrations, for both cases, the initial

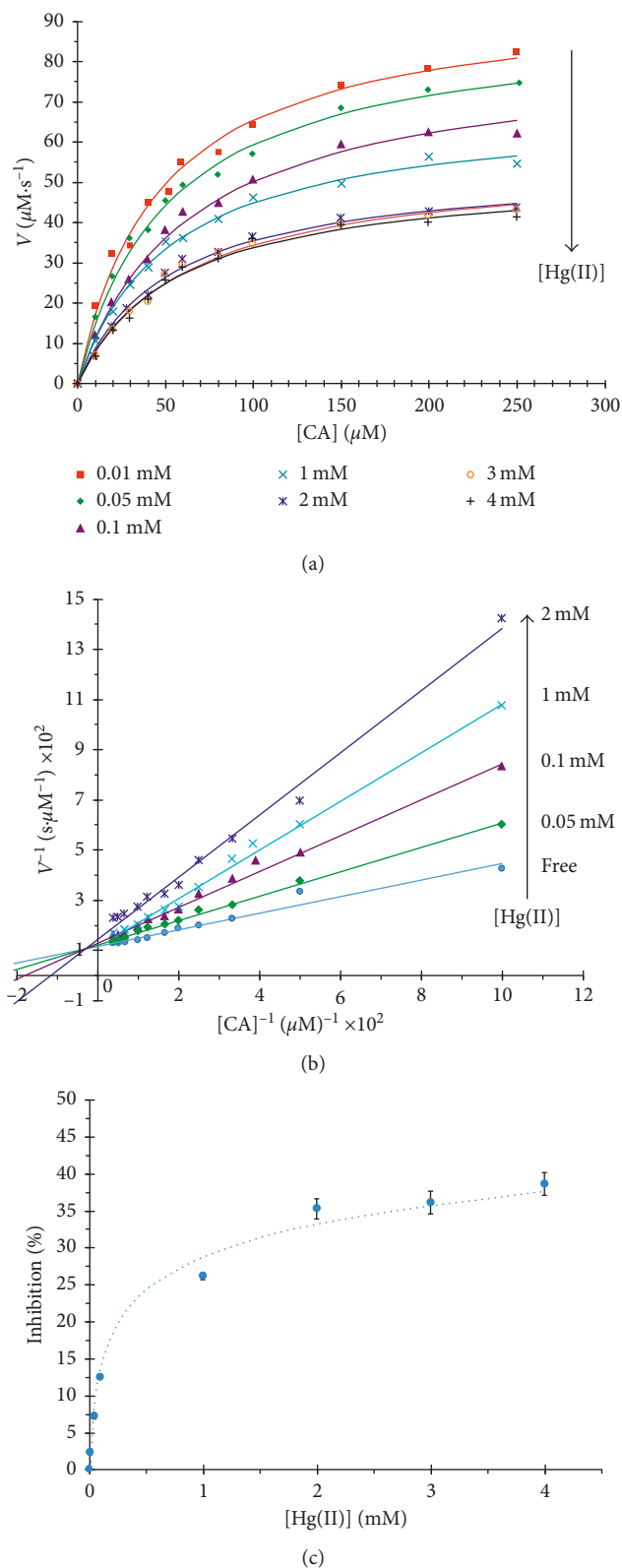


FIGURE 3: (a) Enzymatic reaction rate as a function of CA concentration for different mercury(II) concentrations; (b) double-reciprocal plot ( $1/V$  versus  $1/[\text{CA}]$ ) for the system TvL-CA inhibited for different Hg (II) concentrations; (c) inhibition percent plot of the system TvL-CA at  $200\ \mu\text{M}$  of CA and 2-minute incubation.

TABLE 2: Kinetic parameters for the system TvL-CA as a function of the mercury(II) concentration ( $n = 3$ ).

$[\text{Hg(II)}]$ (mM)	$K_m$ ( $\mu\text{M}$ )	$V_{\max}$ ( $\mu\text{M}\cdot\text{s}^{-1}$ )	$K_{\text{cat}}$ ( $\mu\text{MmL}\cdot\mu\text{g}^{-1}$ )	$k_{\text{cat}}/K_m$ ( $\text{mL}\cdot\mu\text{g}^{-1}$ )
0	$43 \pm 4$	$90 \pm 3$	$9.0 \pm 0.3$	$0.28 \pm 0.03$
0.01	$46 \pm 3$	$95 \pm 3$	$9.5 \pm 0.2$	$0.20 \pm 0.01$
0.05	$49 \pm 3$	$88 \pm 2$	$8.8 \pm 0.3$	$0.20 \pm 0.02$
0.1	$57 \pm 4$	$79 \pm 2$	$7.9 \pm 0.2$	$0.13 \pm 0.01$
1	$53 \pm 4$	$54 \pm 2$	$5.4 \pm 0.2$	$0.11 \pm 0.01$
2	$55 \pm 5$	$53 \pm 2$	$5.3 \pm 0.2$	$0.10 \pm 0.01$
3	$56 \pm 6$	$52 \pm 5$	$5.2 \pm 0.5$	$0.09 \pm 0.01$
4	$54 \pm 5$	$53 \pm 3$	$5.3 \pm 0.3$	$0.10 \pm 0.01$

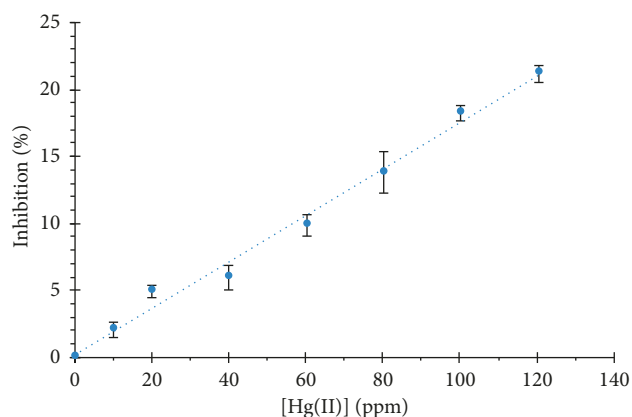


FIGURE 4: Calibration plot for the initial oxidation rate of  $200\ \mu\text{M}$  CA per  $10\ \text{TvL}\cdot\mu\text{g}\cdot\text{mL}^{-1}$  as a function of mercury concentration. The kinetics were obtained in acetate buffer (0.1 M, pH 4.5), monitoring the enzymatic oxidation of CA at 410 nm with 2-minute incubation.

TABLE 3: Percent recoveries for the mercury determination in synthetic samples ( $n = 3$ ).

$[\text{Hg(II)}]_0$ (ppm)	Inhibition (%)	$[\text{Hg(II)}]_{\text{rec.}}$ (ppm)	Recovery %
30	$5.4 \pm 0.3$	$30 \pm 2$	$100 \pm 3.3$
110	$18.5 \pm 0.4$	$106 \pm 6$	$96.4 \pm 5.4$
200	$29.1 \pm 1.4$	$160 \pm 14$	$80.0 \pm 7.0$

rates are small as compared with those of the CA, which exhibits high rates at small concentrations. Therefore, the CA was chosen as the substrate for all subsequent studies.

**3.1. Inhibition Time.** In order to enable an adequate proposal for the same incubation time for TvL inhibition by Hg (II) ions, a study was carried out at 2-, 5-, and 10-minute incubation with constant concentrations of 1 mM mercury. The results are shown in Figure 2, where it can be graphically observed that the kinetic behaviors did not display a significant change for the studied inhibition times. It can also be observed that the 1 mM mercury concentration was capable of inhibiting by about 25% of the catalytic activity of

TABLE 4: Indirect analytical methods for quantification of Hg(II) found in the literature that are based on the principle of enzymatic inhibition.

	Detection method	LOD (ppm)	Linear interval (ppm)	pH	Incubation time (min)	Comment	Ref.
Invertase biosensor	Amperometric	0.001	0.01–0.04	0.1 M NaOH	10	Biosensor coupled to a batch injection analysis	[32]
Invertase immobilized	Thermometric	0.005	0.005–0.08	7.0	2–6	Coupling to FIA	[33]
GOx biosensor	Amperometric	0.05	2–32	7.0	—	Nafion- and MnO <sub>2</sub> -modified CPE	[34]
Invertase-mutarotase-GOx biosensor	Conductimetric	0.005	—	6.5	10–20	—	[35]
GOx free	Colorimetric	0.015	0.005–1	5.0	2	—	[36]
Alcohol ox. and horseradish peroxidase free	Fluorescence	$2.5 \times 10^{-6}$	$5.0 \times 10^{-6}$ –0.05	7.5	20	—	[37]
Sucrose biosensor	Amperometric	—	0.002–0.2	6.0	20	—	[38]
GOx biosensor	Amperometric	—	—	7.0	30	—	[39]
GOx and laccase biosensor	Amperometric	0.03	—	5.0	—	—	[40]
GOx	Amperometric	0.5	0.4–36	7.0	—	—	[41]
Laccase free	Colorimetric	15	10–120	4.5	2	—	This work

the TvL. The Michaelis–Menten ( $K_m$ ) constants for the different inhibition times are shown in Table 1 together with their maximal rates ( $V_{max}$ ), the catalytic constants ( $K_{cat}$ ), and the catalytic efficiencies ( $k_{cat}/K_m$ ). All these values show that there is no meaningful difference among the different inhibition times since all the constant values are statistically equal. Therefore, 2-minute incubation will be the contact time for the forthcoming sections.

**3.2. Effect of the Inhibitor Concentration.** Figure 3(a) shows the effect of the mercury ion concentrations on the TvL catalytic efficiency as a function of varying concentrations of the metal ion (0–4 mM). The enzyme contact time with the inhibitor was 2 minutes for all concentrations with  $10 \mu\text{g}\cdot\text{mL}^{-1}\cdot\text{TvL}$ , for each experiment. It can be clearly noted that the mercury concentration increments resulted in  $V_{max}$  decrements (Figure 3(a) and Table 2). Further, the Michaelis–Menten constant increased lightly, which indicates a mixed inhibition mechanism [30, 31]. In order to further clarify this inhibition mechanism, the Lineweaver–Burk double-reciprocal plots were evaluated for different inhibitor concentrations (Figure 3(b)).

The convergence of the data series on the  $y$ -axis of the Lineweaver–Burk plots is typical of a competitive inhibition mechanism, in which the value of  $K_m$  increases although  $V_{max}$  does not, whereas the data convergence on the  $x$ -axis indicates a noncompetitive mechanism, which in this case  $K_m$  does not change, but  $V_{max}$  diminishes. The analyses of the Lineweaver–Burk double-reciprocal plots indicate that the mercury inhibition mechanism by TvL is carried out through a mix of the previous models (mixture of the competitive and noncompetitive). However, the nonlinear regressions (Figure 3(a) and Table 2) seem to suggest that the inhibition model is closer to the non-competitive model. It can also be observed from Figure 3(c) that a mercury concentration of 0.05 mM inhibited the enzymatic response to 7% and the 0.1 mM concentration

did so to 12%, whereas the 1 mM concentration inhibited to 25%. Lastly, for 2, 3, and 4 mM metal concentrations, an inhibition of approximately 35% was attained without significant change.

Table 2 shows the enzymatic activity parameters for TvL after being inhibited with different mercury ion concentrations, from which it can be said that, at 2, 3, and 4 mM inhibitor concentrations, effectively the response remains constant. Also, the Michaelis–Menten constant shows a small increase with the mercury concentration, and from 2 mM mercury, it is statistically identical. As expected, the maximum rate value decreases with increasing inhibitor concentration, which proves also that the enzyme is being inhibited. It can also be noted that the catalytic constant ( $k_{cat}$ ) and the catalytic efficiency ( $k_{cat}/K_m$ ) diminish with increasing mercury concentration until it remained constant at higher inhibitor concentrations. All these results reveal the possibility to use the TvL inhibition for the mercury(II) quantification in aqueous solution.

### 3.3. Mercury(II) Determination in Synthetic Samples.

Several calibration plots were built in order to determine mercury(II) in synthetic samples as a function of the metal ion concentration, keeping the TvL concentration constant at  $10 \mu\text{g}\cdot\text{mL}^{-1}$  and 2 minutes in contact with the inhibitor. For this test, synthetic mercury solutions containing 30, 110, and 200 ppm were prepared by dissolving mercury nitrate in deionized water. Figure 4 shows the calibration plot; the method rendered a detection limit of  $15 \pm 1$  ppm and a linear range of 10 to 120 ppm. The detection limit (DL) was calculated using the equation  $DL = 3s_y/m_{cal}$ , where  $s_y$  represents the typical error and  $m_{cal}$  represents the slope of the calibration plot. A summary of the results of the mercury(II) determination in synthetic samples is shown in Table 3. For mercury concentrations of 30, 110, and 200 ppm, the percent recovery were as follows: 100, 96.4, and 80.0%, respectively, with errors smaller than 7%.

**3.4. Comparison with the Literature.** Table 4 shows a comparison between the methods proposed in the literature and that described in the present work for determining mercury(II) in aqueous solution, all of them based on the same enzymatic inhibition principle. It is worthwhile to state that there are only a few methods based on this principle of using free enzymes (not immobilized).

Conversely, there are numerous methods reported using enzymes immobilized on a polymer network to modify Pt, Au, glassy carbon, carbon paste, and printed electrodes, among others. It is also important to point out that a large number of works have used enzymes such as glucose oxidase (GOx), invertase, urease, and others, to be inhibited by mercury, although laccase has been much less studied. The method reported here is comparable with some other methods reported insofar as their detection limit, even though this is not the case for the majority of them, because they report detection limits inferior to those in this work. However, the method reported here presents other advantages because the enzyme is free in solution, apart from the fact that the amount of laccase needed for each analysis is very small ( $10 \mu\text{g}\cdot\text{mL}^{-1}$ ) as well as the buffer solution (2 mL), and lastly, the analysis cost is indeed small, because they are coupled to a quick and simple procedure.

#### 4. Conclusions

The laccase enzymatic inhibition through mercury(II) ions was reported, establishing a mixed inhibition model (preferable to a noncompetitive inhibition model) by means of UV-Vis spectrophotometry. The TvL enzyme presents higher activity when using caffeic acid as a substrate, in comparison with gallic acid and catechol, fitting in the Michaelis–Menten with constants of  $43 \pm 4$ ,  $85 \pm 1$ , and  $307 \pm 18 \mu\text{M}$ , respectively. Small mercury(II) ion concentrations did inhibit the TvL enzymatic activity in only 2 contact minutes, without meaningful difference at greater times. Then, the mercury laccase inhibition was used for quantification of the metal ion. The method reported here exhibited a detection limit of  $15 \pm 1$  ppm with a linear dynamic interval of 10–120 ppm mercury ( $R^2 = 0.9893$ ). Further, the method is fast and simply implemented into other procedures of environmental remediation.

#### Data Availability

The data used to support the findings of this study are available from the corresponding author upon request.

#### Conflicts of Interest

There are no conflicts to declare.

#### Acknowledgments

Rosas-Tate thanks CONACYT for the grant given for the master's degree. J. Juárez-Gómez, G. Roa-Morales, P. Balderas-Hernández, M. Romero-Romo, and M.T. Ramírez-Silva wish to thank the SNI for the distinction of their

membership and the stipend received. The authors thank the UAEM for financial support through Project 3736/2014/CID. MTRS and J. Juárez-Gómez thank CONACYT for the “Cátedra” 2159 and for support through Project 237327.

#### References

- [1] C. M. Rivera-Hoyos, E. D. Morales-Álvarez, R. A. Poutou-Piñales, A. M. Pedroza Rodríguez, R. Rodríguez-Vázquez, and J. M. Delgado-Boada, “Fungal laccases,” *Fungal Biology Reviews*, vol. 27, no. 3-4, pp. 67–82, 2013.
- [2] U. N. Dwivedi, P. Singh, V. P. Pandey, and A. Kumar, “Structure-function relationship among bacterial, fungal and plant laccases,” *Journal of Molecular Catalysis B: Enzymatic*, vol. 68, no. 2, pp. 117–128, 2011.
- [3] A. Messerschmidt, L. Mander, and H. W. Liu, *Comprehensive Natural Products II, Chemistry and Biology*, Elsevier Oxford, Italy, 2010.
- [4] H. Catherine, M. Penninckx, and D. Frédéric, “Product formation from phenolic compounds removal by laccases: a review,” *Environmental Technology and Innovation*, vol. 5, pp. 250–266, 2016.
- [5] J. A. Majeau, S. K. Brar, and R. D. Tyagi, “Laccases for removal of recalcitrant and emerging pollutants,” *Bioresource Technology*, vol. 107, no. 7, pp. 2331–2350, 2010.
- [6] C. F. Thurston, “The structure and function of fungal laccases,” *Microbiology*, vol. 140, no. 1, pp. 19–26, 1994.
- [7] E. I. Solomon, U. M. Sundaram, and T. E. Machonkin, “Multicopper oxidases and oxygenases,” *Chemical Reviews*, vol. 96, no. 7, pp. 2563–2606, 1996.
- [8] I. Bento, M. A. Carrondo, and P. F. Lindley, “Reduction of dioxygen by enzymes containing copper,” *Journal of Biological Inorganic Chemistry*, vol. 11, no. 5, pp. 539–547, 2006.
- [9] E. I. Solomon, M. J. Baldwin, and M. D. Lowery, “Electronic structures of active sites in copper proteins: contributions to reactivity,” *Chemical Reviews*, vol. 92, no. 4, pp. 521–542, 1992.
- [10] P. Baldrian, “Purification and characterization of laccase from the white-rot fungus *Daedalea quercina* and decolorization of synthetic dyes by the enzyme,” *Applied Microbiology and Biotechnology*, vol. 63, no. 5, pp. 560–563, 2004.
- [11] X. Hu, C. Wang, L. Wang, R. Zhang, and H. Chen, “Influence of temperature, pH and metal ions on guaiacol oxidation of purified laccase from *Leptographium qinlingensis*,” *World Journal of Microbiology and Biotechnology*, vol. 30, no. 4, pp. 1285–1290, 2014.
- [12] L. Gianfreda, F. Xu, and J. M. Bollag, “Laccases: a useful group of oxidoreductive enzymes,” *Bioremediation Journal*, vol. 3, no. 1, pp. 1–26, 1999.
- [13] K. Hailemariam, P. M. Bolger, and Y. Motarjemi, *Toxic Metals: Mercury*, Academic Press, Cambridge, MA, USA, 2014.
- [14] OMS. *Mercurio y Salud*, 2016, <http://www.who.int/mediacentre/factsheets/fs361/en/>.
- [15] J. Pletz, F. Sánchez-Bayo, and H. A. Tennekes, “Dose-response analysis indicating time-dependent neurotoxicity caused by organic and inorganic mercury—implications for toxic effects in the developing brain,” *Toxicology*, vol. 347–349, pp. 1–5, 2016.
- [16] H. C. Hsi, C. B. Jiang, T. H. Yang, and L. C. Chien, “The neurological effects of prenatal and postnatal mercury/methylmercury exposure on three-year-old children in Taiwan,” *Chemosphere*, vol. 100, pp. 71–76, 2014.
- [17] A. J. Clarke and L. S. Adams, “Irreversible inhibition of *Schizophyllum commune* cellulase by divalent transition metal

- ions," *Biochimica et Biophysica Acta (BBA)-Protein Structure and Molecular Enzymology*, vol. 916, no. 2, pp. 213–219, 1987.
- [18] D. Mealor and A. Townshend, "Applications of enzyme-catalysed reactions in trace analysis," *Talanta*, vol. 15, no. 8, pp. 747–758, 1968.
- [19] M. Michelin, T. M. Silva, V. M. Benassi, S. C. Peixoto-Nogueira, L. A. B. Moraes, and J. M. Leão, "Purification and characterization of a thermostable  $\alpha$ -amylase produced by the fungus *Paecilomyces variotii*," *Carbohydrate Research*, vol. 345, no. 16, pp. 2348–2353, 2010.
- [20] P. Gupta, M. Jain, J. Sarangthem, and R. Gadre, "Inhibition of 5-aminolevulinic acid dehydratase by mercury in excised greening maize leaf segments," *Plant Physiology and Biochemistry*, vol. 62, pp. 63–69, 2013.
- [21] L. A. O. Silva, C. R. F. Terrasan, and E. C. Carmona, "Purification and characterization of xylanases from *Trichoderma inhamatum*," *Electronic Journal of Biotechnology*, vol. 18, no. 4, pp. 303–313, 2015.
- [22] P. Ibarra-Escutia, J. Juarez Gómez, C. Calas-Blanchard, J. L. Marty, and M. T. Ramírez-Silva, "Amperometric biosensor based on a high resolution photopolymer deposited onto a screen-printed electrode for phenolic compounds monitoring in tea infusions," *Talanta*, vol. 81, no. 4-5, pp. 1636–1642, 2010.
- [23] E. Rodríguez-Sevilla, M. T. Ramírez-Silva, M. Romero-Romo, P. Ibarra-Escutia, and M. Palomar-Pardavé, "Electrochemical quantification of the antioxidant capacity of medicinal plants using biosensors," *Sensors*, vol. 14, no. 8, p. 14423, 2014.
- [24] D. F. Swinehart, "The Beer-Lambert law," *Journal of Chemical Education*, vol. 20, no. 7, pp. 333–335, 1962.
- [25] K. A. Johnson, "A century of enzyme kinetic analysis," *FEBS Letters*, vol. 587, no. 17, pp. 2153–2766, 2013.
- [26] M. L. Cárdenas, "Michaelis and Menten and the long road to the discovery of cooperativity," *FEBS Letters*, vol. 587, no. 17, pp. 2767–2771, 2013.
- [27] A. Cornish-Bowden, "The origins of enzyme kinetics," *FEBS Letters*, vol. 587, no. 17, pp. 2725–2730, 2013.
- [28] A. Cornish-Bowden, "One hundred years of Michaelis-Menten kinetics," *Perspectives in Science*, vol. 4, pp. 3–9, 2015.
- [29] G. Wang and W. M. Post, "A note on the reverse Michaelis-Menten kinetics," *Soil Biology and Biochemistry*, vol. 57, pp. 946–949, 2013.
- [30] A. Cornish-Bowden, "A simple graphical method for determining the inhibition constants of mixed, uncompetitive and non-competitive inhibitors," *Biochemical Journal*, vol. 137, no. 1, pp. 143–144, 1974.
- [31] H. Lineweaver and D. Burk, "The determination of enzyme dissociation constants," *Journal of the American Chemical Society*, vol. 56, no. 3, pp. 658–666, 1934.
- [32] H. Mohammadi, M. E. Rhazi, A. Amine, A. M. Oliveira Brett, and C. M. A. Brett, "Determination of mercury(II) by invertase enzyme inhibition coupled with batch injection analysis," *Analyst.*, vol. 127, no. 8, pp. 1088–1093, 2002.
- [33] S. Pirvutoiu, I. Surugiu, E. S. Dey, A. Ciucu, V. Magearu, and B. Danielsson, "Flow injection analysis of mercury(II) based on enzyme inhibition and thermometric detection," *Analyst*, vol. 126, no. 9, pp. 1612–1616, 2001.
- [34] A. Samphao, H. Rerkchai, J. Jitcharoen, D. Nacapricha, and K. Kalcher, "Indirect determination of mercury by inhibition of glucose oxidase immobilized on a carbon paste electrode," *International Journal of Electrochemical Science*, vol. 7, pp. 1001–1010, 2012.
- [35] O. O. Soldatkin, I. S. Kucherenko, V. M. Pyeshkova et al., "Novel conductometric biosensor based on three-enzyme system for selective determination of heavy metal ions," *Bioelectrochemistry*, vol. 83, pp. 25–30, 2012.
- [36] A. Ciucu, "Fast spectrometric method for mercury(II) determination based on glucose-oxidase inhibition," *Analytical Letters*, vol. 43, no. 7-8, pp. 1377–1386, 2010.
- [37] K. Deshpande, R. K. Mishra, and S. Bhand, "A high sensitivity micro format chemiluminescence enzyme inhibition assay for determination of Hg(II)," *Sensors*, vol. 10, no. 7, pp. 6377–6394, 2010.
- [38] H. Mohammadi, A. Amine, S. Cosnier, and C. Mousty, "Mercury-enzyme inhibition assays with an amperometric sucrose biosensor based on a trienzymatic-clay matrix," *Analytica Chimica Acta*, vol. 543, no. 1-2, pp. 143–149, 2005.
- [39] C. Malitesta and M. R. Guascito, "Heavy metal determination by biosensors based on enzyme immobilised by electropolymerisation," *Biosensors and Bioelectronics*, vol. 20, no. 8, pp. 1643–1647, 2005.
- [40] S. Cosnier, C. Mousty, A. Guelorget, M. Sanchez-Paniagua Lopez, and D. Shan, "A fast and direct amperometric determination of Hg<sup>2+</sup> by a bienzyme electrode based on the competitive activities of glucose oxidase and laccase," *Electroanalysis*, vol. 23, no. 8, pp. 1776–1779, 2011.
- [41] M. R. Guascito, C. Malitesta, E. Mazzotta, and A. Turco, "Inhibitive determination of metal ions by an amperometric glucose oxidase biosensor: Study of the effect of hydrogen peroxide decomposition," *Sensors and Actuators B: Chemical*, vol. 131, no. 2, pp. 394–402, 2008.



Hindawi

Submit your manuscripts at  
[www.hindawi.com](http://www.hindawi.com)

